Time-dependent pairing equations for seniority-one nuclear systems

M. Mirea

Horia Hulubei National Institute for Physics and Nuclear Engineering, P. O. Box MG-6, 077125 Bucharest-Magurele, Romania

(Received 27 May 2008; revised manuscript received 14 September 2008; published 31 October 2008)

When the time-dependent Hartree-Fock-Bogoliubov intrinsic equations of motion are solved in the case of seniority-one nuclear systems, the unpaired nucleon remains on the same orbital. The blocking effect hinders the possibility to skip from one orbital to another. This unpleasant feature is by-passed with a new set of pairing time-dependent equations that allows the possibility that the unpaired nucleon changes its single-particle level. These equations generalize the time-dependent Hartree-Fock-Bogoliubov equations of motion by including the Landau-Zener effect. The derivation of these new equations is presented in detail. These equations are applied to the case of a superasymmetric fission process, that is, to explain the fine structure the ^{14}C emission from ^{233}Ra. In this context, a new version of the Woods-Saxon model extended for two-center potentials is used.

DOI: 10.1103/PhysRevC.78.044618 PACS number(s): 24.10.Eq, 21.30.Fe, 23.70.+j, 27.90.+b

I. INTRODUCTION

In the Hartree-Fock (HF) approximation, the self-consistent potential for heavy nuclei is quite smooth, since it includes the convolution of many instantaneous densities. If the potential varies in time, each single-particle wave function moves independently in the smoothly varying well. The Pauli principle is fulfilled, being mediated permanently through the mean field potential. The two-body collisions are incorporated in the equations of motion only to the extent to which they contribute to the mean field. In principle, the time-dependent HF approach exactly treats the residual interactions only if the mean field is allowed to break all symmetries. Such HF descriptions that allow breaking symmetries have been reported, for example, in investigating the excitation functions of the $^{16}\mathrm{O} + {}^{205}\mathrm{Pb}$ system [1], in studying the isovector giant dipole resonance state in the continuum for ^{16}O [2], in describing static properties and reaction rates [3], and in computing dipole strength distributions [4]. However, such an approach leads to a huge computational problem. Because of these difficulties, as mentioned in Ref. [5], even in the global mass fit strategy, HF codes are restricted to being either spherical or axially symmetrical with reflection invariant shapes. Usually, the HF mean field is constrained to be at least axially symmetric. In this case, levels characterized by the same good quantum numbers cannot intersect. In such circumstances, when the equations of motion are solved, an individual single-particle wave function will belong to only one orbital characterized by some good quantum numbers, and the mechanism of level slippage [6] is not allowed. In general, two dynamical approaches are used. On one hand, the generator coordinate method assumes that the internal structure of the decaying system is equilibrated at each step of the collective motion [7]. On the other hand, the exchange between collective and internal degrees of freedom is neglected [8], so that adiabaticity is assumed. Usually, this behavior leads to the unpleasant feature that a system, even moving infinitely slowly, could not end up in its ground state. Some attempts were done to extend the time-dependent HF method in order to include collision terms [9–11]. Such approaches were developed and led to the extended mean field model and the time-dependent stochastic Hartree-Fock equations discussed in detail in Refs. [12,13]. Alternatively, this problem was partially solved in the 1980s by introducing a residual pairing interaction in the time-dependent Hartree-Fock-Bogoliubov (TDHFB) approach [14–16]. This method provides the possibility of level slippage for pairs and allows a description of the nuclear dynamics. For example, in the case of an even-even system, this approach represents a tool for estimating dissipation during disintegration processes [14,17]. A deep connection with the Landau-Zener effect is included in the TDHFB equations; pairs undergo Landau-Zener transitions on virtual levels with coupling strengths given by the magnitude of the gap Δ [16]. Unfortunately, for seniority-one nuclear systems, the pairing residual interaction does not affect a single nucleon; and during the deformation of the nucleus from its initial state up to scission, the unpaired particle remains located on the same orbital. The level slippage is again forbidden for the blocked level.

In the case of independent single particles, by neglecting residual interactions, the problem of the unpaired nucleon is solved in terms of the Landau-Zener effect. The Landau-Zener effect reflects a mechanism that allows the possibility that a single nucleon skips from one single-particle level to another one in some avoided level crossing regions. The probabilities that the unpaired nucleon arrives in different final states can be computed by solving a system of coupled-channel equations that characterizes the microscopic motion. In this work, a way to introduce a similar mechanism for the unpaired nucleon in superfluid systems is investigated. The TDHFB equations will be generalized to include the Landau-Zener effect. The classical TDHFB equations and the equations that govern the Landau-Zener effect will be obtained as particular cases of the new time-dependent pairing equations.

For compatibility with most publications done in the past, the terminology TDHFB is used for the time-dependent pairing (or BCS) equations. It must be pointed out that the equations of motion derived in the following are compatible only within the HF+BCS theory. The technique of the full consistent TDHFB theory is much more complex and was addressed recently in Refs. [18,19].

 ©2008 The American Physical Society

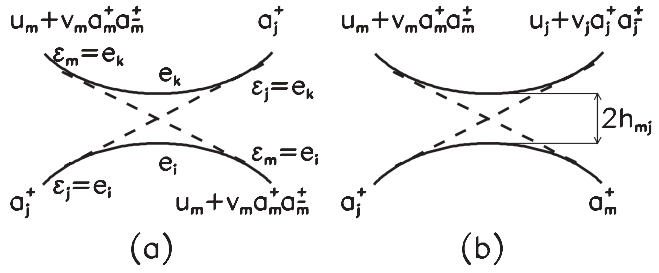

FIG. 1. Ideal avoided crossing region and possible transition states for an unpaired nucleon in the superfluid model. (a) The single particle follows the diabatic level. (b) The single particle remains on the same adiabatic state.

II. LANDAU-ZENER EFFECT

Single-particle levels are functions of the deformation parameters that characterize the shape of a nucleus. Levels characterized by the same quantum numbers associated with some symmetry of the system cannot cross and exhibit avoided level crossings. The transition probability of a nucleon from one adiabatic level to another is strongly enhanced in an avoided crossing region. This promotion mechanism is known as the Landau-Zener effect [6].

In Fig. 1(a), an ideal avoided crossing (j, m) between two adiabatic levels e_k and e_i is displayed. The diabatic levels are ϵ_m and ϵ_j. If the variation of the generalized coordinate is produced slowly and the nucleon is initially located on the level e_i, after the passage of the avoided crossing region, the nucleon will practically remain on the same adiabatic level. In this case, the motion is adiabatic, and the nucleon follows the adiabatic state e_i. If the variation of the generalized coordinate is produced suddenly, then the nucleon will skip with a large probability on the adiabatic level e_k. Then the motion is diabatic, and the nucleon follows the diabatic state ϵ_j. A formalism can be used to obtain the promotion probability. Assuming an n-state approximation, the wave function of the unpaired nucleon can be formally expanded in a basis of n diabatic wave functions $\psi_i(r)$ as

$$\Psi(r,t) = \sum_i^n c_i(t)\psi_i(r)\exp\left(-\frac{i}{\hbar}\int_0^t \epsilon_i(\tau)\,d\tau\right), \qquad (1)$$

where the matrix elements with the diabatic states are $\epsilon_i = \langle\psi_i|H|\psi_i\rangle$ and $h_{ij} = \langle\psi_i|H|\psi_j\rangle = h_{ji}$. H is the mean field Hamiltonian and c_i are amplitudes. Inserting the wave function (1) in the time-dependent Schrödinger equation, the following system of coupled equations is obtained:

$$\dot{c}_i(t) = \frac{1}{i\hbar}\sum_{j\neq i}^n c_j(t)h_{ij}(t)\exp\left(-\frac{i}{\hbar}\int_0^t(\epsilon_j(\tau)-\epsilon_i(\tau))\,d\tau\right). \qquad (2)$$

Here, $p_i = |c_i|^2$ is the probability of finding the unpaired nucleon on the level i.

These equations have already been used to explain the resonant-like structure of the inelastic cross sections in heavy-ion collisions [20,21], the fine structure in cluster emission [22,23] and in α decay [24], and the resonant structure in the fission cross section [25–27].

III. SUPERFLUID SYSTEMS

An effect analogous to the Landau-Zener one can be obtained by generalizing the TDHFB equations for the case of seniority-one nuclear systems. The problem will be explored in the simplest possible way: a monopole pairing force, and a sufficiently weak pairing such that the nucleons are not redistributed to change significantly the mean field potential. The study available in Ref. [28] assessed that the state-independent seniority pairing force becomes unreliable for nuclei close to the drip lines. However, in the neighborhood of the stability valley, the BCS approximation performs remarkably well as evidenced by the global mass fit realized in Ref. [29] or by the comparison between a density-dependent delta interaction and the seniority force in the case of neutron occupation probabilities of Sn single-particle levels [30]. To make the problem tractable, two approaches are investigated. The first one is valid for a low-lying level system with a small number of avoided crossing regions, so that variations of densities ρ_i and pairing moment components κ_i due to the blocked level can be neglected. The second one takes into account the blocking effect, that is, the fact that $\rho_{i(m)}$ and $\kappa_{i(m)}$ depend on the blocked level m.

A. Low-lying levels

Using quasiparticle creation and annihilation operators $\alpha_{\bar{k}}^+$ and $\alpha_{\bar{k}}$

$$\begin{aligned}\alpha_k &= u_k a_k - v_k a_{\bar{k}}^+,\\ \alpha_{\bar{k}} &= u_k a_{\bar{k}} + v_k a_k^+,\\ \alpha_k^+ &= u_k a_k^+ - v_k^* a_{\bar{k}},\\ \alpha_{\bar{k}}^+ &= u_k a_{\bar{k}}^+ + v_k^* a_k,\end{aligned} \qquad (3)$$

it is possible to construct some interactions that help us promote the nucleon from one diabatic level to another. The two situations plotted in Fig. 1 can be modeled. In plot (a), the single particle follows the diabatic level ϵ_j, while in plot (b) it remains on the adiabatic one e_i. Here a_k^+ and a_k denote operators for creating and destroying a particle in the state k, respectively. The state characterized by a bar signifies the time-reversed partner of a pair. The parameters v_k and u_k are the occupation and vacancy amplitudes, respectively. Because only the relative phase between the parameters u_k and v_k matters, in the following, u_k is considered to be a real quantity and v_k a complex one. The interaction able to promote the unpaired nucleon from one adiabatic level to another must be given by some products of operators of the type in Eq. (3).

To obtain the equations of motion, we shall start from the variational principle taking the following energy functional

$$\delta L = \delta\langle\varphi|H - i\hbar\frac{\partial}{\partial t} + H' - \lambda N|\varphi\rangle, \qquad (4)$$

and assuming the many-body state formally expanded as a superposition of n time-dependent BCS seniority-one diabatic wave functions

$$|\varphi(t)\rangle = \sum_m^n c_m(t)a_m^+\prod_{l\neq m}(u_l(t) + v_l(t)a_l^+a_{\bar{l}}^+)|0\rangle. \qquad (5)$$

Sometimes, this energy functional is called a Lagrangian [16, 31]. The functional contains several terms. The first one is the many-body Hamiltonian with pairing residual interactions

$$H(t) = \sum_{k>0} \epsilon_k(t)(a_k^+ a_k + a_{\bar{k}}^+ a_{\bar{k}}) - G \sum_{k,l>0} a_k^+ a_{\bar{k}}^+ a_l a_{\bar{l}}. \quad (6)$$

The residual interactions between diabatic levels characterized by the same quantum numbers that are responsible for the Landau-Zener effect are assumed on the form

$$\begin{aligned} H'(t) &= \sum_{i,j\neq i}^{n} h_{ij}(t)\alpha_i^+ \alpha_j \\ &= \sum_{i,j\neq i}^{n} h_{ij}(t)(u_i a_i^+ - v_i^* a_{\bar{i}})(u_j a_j - v_j a_{\bar{j}}^+). \end{aligned} \quad (7)$$

The sum runs over diabatic levels i and j. The particle number operator is

$$N = \sum_{k>0} (a_k^+ a_k + a_{\bar{k}}^+ a_{\bar{k}}). \quad (8)$$

After some calculations, as detailed in Appendix A, the next system of time-dependent coupled-channel equations are obtained [32]:

$$i\hbar\dot{\rho}_l = \sum_{m}^{n} p_m\{\kappa_l \Delta_m^* - \kappa_l^* \Delta_m\}, \quad (9)$$

$$i\hbar\dot{\kappa}_l = \sum_{m}^{n} p_m\{(2\rho_l - 1)\Delta_m + 2\kappa_l(\epsilon_l - \lambda) - 2G\rho_l\kappa_l\}, \quad (10)$$

$$i\hbar\dot{p}_m = \sum_{j\neq m}^{n} h_{mj}(S_{mj} - S_{jm}), \quad (11)$$

$$\begin{aligned} i\hbar\dot{S}_{jm} = S_{jm}\Bigg\{ & -\frac{1}{G}\left(|\Delta_m|^2 - |\Delta_j|^2\right) + (\epsilon_m(t) - \epsilon_j(t)) \\ & - G\left(\rho_m^2 - \rho_j^2\right) - \frac{1}{2}\left(-\frac{\rho_m}{\kappa_m} + 2\kappa_m^* + \frac{\rho_j}{\kappa_j} - 2\kappa_j^*\right) \\ & \times \sum_{l}^{n} p_l \Delta_l - \frac{1}{2}\left(-\frac{\rho_m}{\kappa_m^*} + 2\kappa_m + \frac{\rho_j}{\kappa_j^*} - 2\kappa_j\right) \\ & \times \sum_{l}^{n} p_l \Delta_l^* \Bigg\} + \sum_{l\neq m,j}^{n} [h_{ml}(t)S_{jl} - h_{jl}(t)S_{lm}] \\ & + h_{mj}(t)(p_j - p_m). \end{aligned} \quad (12)$$

Here, the following notations are used:

$$\begin{aligned} \Delta_m &= G\sum_{k\neq m} \kappa_k, \\ \Delta_m^* &= G\sum_{k\neq m} \kappa_k^*, \\ \kappa_k &= u_k v_k, \\ \rho_k &= |v_k|^2, \\ p_m &= |c_m|^2, \\ S_{jm} &= c_j^* c_m, \end{aligned} \quad (13)$$

where ρ_k are the single-particle densities, κ_k are the pairing moment components, and p_m denotes the probability to have an unpaired nucleon on the level m. ρ_k and p_m are real quantities, while κ_k and S_{jm} are complex ones. In analogy with the pairing moment components κ_k, S_{jm} can be called unpairing moment components, having the property $|S_{jm}|^2 = p_j p_m$. Whenever the upper limit n is specified for a sum, it is implicitly assumed that the operation is realized on the n possible diabatic states of the unpaired nucleon. In this paper, the sum over pairs generally runs over the index k. When the single-particle sum over k is realized only for one partner of each reversed pair, the result is multiplied by a factor of 2. The index k runs over a workspace that allows the pairing force to operate only within a finite number of active levels around the Fermi energy.

B. Blocking effect

If the blocking effect is taken into consideration, each seniority-one BCS wave function is characterized by its own set of ρ and κ values, and the trial wave function is

$$|\varphi(t)\rangle = \sum_{m}^{n} c_m(t) a_m^+ \prod_{l\neq m} (u_{l(m)}(t) + v_{l(m)}(t) a_l^+ a_{\bar{l}}^+)|0\rangle. \quad (14)$$

The Landau-Zener interaction is postulated as

$$\begin{aligned} H'(t) &= \sum_{i,j\neq i}^{n} h_{ij}(t)\alpha_{i(j)}^+ \alpha_{j(i)} \prod_{k\neq i,j} \alpha_{k(j)} a_k^+ a_k \alpha_{k(i)}^+ \\ &= \sum_{i,j\neq j}^{n} h_{ij}(t)(u_{i(j)} a_i^+ - v_{i(j)}^* a_{\bar{i}})(u_{j(i)} a_j + v_{j(i)} a_{\bar{j}}^+) \\ &\quad \times \prod_{k\neq i,j} \alpha_{k(j)} a_k^+ a_k \alpha_{k(i)}^+, \end{aligned} \quad (15)$$

where the quasiparticle creation and annihilation operators

$$\begin{aligned} \alpha_{k(j)} &= u_{k(j)} a_k - v_{k(j)} a_{\bar{k}}^+, \\ \alpha_{\bar{k}(j)} &= u_{k(j)} a_{\bar{k}} + v_{k(j)} a_k^+, \\ \alpha_{k(j)}^+ &= u_{k(j)} a_k^+ - v_{k(j)}^* a_{\bar{k}}, \\ \alpha_{\bar{k}(j)}^+ &= u_{k(j)} a_{\bar{k}}^+ + v_{k(j)}^* a_k, \end{aligned} \quad (16)$$

are now associated with each blocked level (j). This kind of interaction describes the full phenomenon only in an approximate way. In this context, if a diabatic wave function i is "reflected" in an avoided crossing region (i, j), this wave function is transformed in a component of the diabatic wave function j. However, the reality is more complicated. When a diabatic wave function i is reflected in an avoided crossing region, this wave function must be split into two parts: a transmitted diabatic wave function i and a reflected adiabatic wave function j'. That means, the number of wave functions must be doubled after the passage of each avoided crossing region. Therefore, in treating the more realistic situations, the system of coupled-channel equations becomes much more complicated. For simplicity, in our approximations, we considered only a superposition of n diabatic wave functions;

that means, the diabatic wave function i is forced to contribute to the amplitude of the diabatic wave function j (which is not always equivalent to j'). After some calculation, as detailed in Appendix B, a new set of pairing equations that accounts for configuration mixing results:

$$i\hbar\dot{\rho}_{l(m)} = \kappa_{l(m)}\Delta_m^* - \kappa_{l(m)}^*\Delta_m, \tag{17}$$

$$i\hbar\dot{\kappa}_{l(m)} = (2\rho_{l(m)} - 1)\Delta_m + 2\kappa_{l(m)}(\epsilon_l - \lambda_m) - 2G\rho_{l(m)}\kappa_{l(m)}, \tag{18}$$

$$i\hbar\dot{p}_m = \sum_{j\neq m}^{n} h_{mj}(S_{mj} - S_{jm}), \tag{19}$$

$$\begin{aligned} i\hbar\dot{S}_{jm} = S_{jm}\Bigg\{ & -\frac{1}{G}\left(|\Delta_m|^2 - |\Delta_j|^2\right) \\ & + (\epsilon_m(t) - \epsilon_j(t) - \lambda_m + \lambda_j) \\ & + G\left(\sum_{k\neq m}\rho_{k(m)}^2 - \sum_{k\neq j}\rho_{k(j)}^2\right) \\ & - \frac{1}{2}\sum_{k\neq m}(\Delta_m\kappa_{k(m)}^* + \Delta_m^*\kappa_{k(m)})\left(\frac{\rho_{k(m)}^2}{|\kappa_{k(m)}|^2} - 1\right) \\ & + \frac{1}{2}\sum_{k\neq j}(\Delta_j\kappa_{k(j)}^* + \Delta_j^*\kappa_{k(j)})\left(\frac{\rho_{k(j)}^2}{|\kappa_{k(j)}|^2} - 1\right)\Bigg\} \\ & + \sum_{l\neq m,j}^{n}[h_{ml}(t)S_{jl} - h_{jl}(t)S_{lm}] + h_{mj}(t)(p_j - p_m). \end{aligned} \tag{20}$$

Here, the same notations as in the previous approach are used.

Two main differences arise between Eqs. (9)–(12) and (17)–(20) that are implicitly determined by the hypothesis assumed in their derivation. First, in Eqs. (9)–(12) the values of $\dot{\rho}$ and $\dot{\kappa}$ are obtained through a weighted sum that runs over unpaired states, while in Eqs. (17) and (18) these quantities belong to only one diabatic wave function. Second, in Eq. (20), $\dot{S_{jm}}$ depends on all densities ρ and pairing moment components κ of the implied two diabatic wave functions j and m. As a consequence of these differences, the number of differential equations increases n times in Eqs. (17) and (18). Another consequence is that $2\sum_{k\neq m}\rho_{k(m)} = N - 1$ for each diabatic wave function m in Eqs. (17) and (18), while $2\sum_k \rho_k = N + 2\rho_F - 1$ in Eqs. (9)–(12), where ρ_F denotes the occupation number associated with the Fermi level in the initial ground state configuration. Finally, the chemical potential λ has values associated with the diabatic state under consideration in Eqs. (17) and (18).

IV. ENERGY

In this section, only the equations associated with the blocking level approach are displayed. For the low-lying level approach, the index (m) must be dropped. The ground state energy E_0 of any deformation is obtained in the framework of the BCS formalism by considering that the Fermi level ϵ_F is populated with the unpaired nucleon, that is,

$$E_0 = 2\sum_{k\neq F}\rho_{k(F)}\epsilon_k + \epsilon_F - G\left|\sum_{k\neq F}\kappa_{k(F)}\right|^2 - G\sum_{k\neq F}\rho_{k(F)}^2, \tag{21}$$

in the static, lower energy state. For the same deformation, the energy of an diabatic state m is obtained by considering the unpaired nucleon located on the diabatic state under consideration,

$$E_m = 2\sum_{k\neq m}\rho_{k(m)}\epsilon_k + \epsilon_m - G\left|\sum_{k\neq m}\kappa_{k(m)}\right|^2 - G\sum_{k\neq m}\rho_{k(m)}^2, \tag{22}$$

where the solutions of the TDHFB equations are used. In the frame of our model, the difference

$$\Delta E_m = E_m - E_0 \tag{23}$$

behaves as a specialization energy. So, as implied in Ref. [33], the quantity ΔE_m must increase the potential barrier tunneled by the nuclear system. Different barriers are obtained for each diabatic state under consideration. These appear as dynamic excitations during the decaying process. Combining excitations with occupation probabilities of diabatic states, we obtain

$$E = \sum_m^n p_m E_m \tag{24}$$

for the average energy and

$$\Delta\bar{E} = \sum_m^n p_m \Delta E_m \tag{25}$$

for the averaged dissipated energy during the decay. As mentioned in Ref. [34], the collective kinetic energy is temporarily stored as a conservative potential. This energy subsequently decays partially in dissipation.

Equations (9)–(12) and (17)–(20) involve only single-particle energies. They conserve the average number of particles, because $2\sum_{k\neq m}\rho_{k(m)} = N - 1$ for any m (or $2\sum_k \rho_k = N + 2\rho_F - 1$) and $\sum_m^n p_m = 1$. The average energy can evolve in time as follows:

$$\begin{aligned} \dot{E} = \sum_m^n p_m \Bigg\{ & 2\sum_{k\neq m}\rho_{k(m)}\dot{\epsilon}_k + \dot{\epsilon}_m \\ & - \dot{G}\left|\sum_{k\neq m}\kappa_{k(m)}\right|^2 - \dot{G}\sum_{k\neq m}\rho_{k(m)}^2\Bigg\}. \end{aligned} \tag{26}$$

For a stationary system, for which $\dot{\epsilon} = 0$ and $\dot{G} = 0$, the total energy is conserved, even if individual values of p, ρ, and κ may still be varying with time. In our treatment, the chemical potential has the values λ_m obtained from BCS equations for each energy level workspace associated with the diabatic wave function m.

Macroscopic approaches can also be used to determine the energy dissipation. The transfer of collective motion energy into internal excitation is evaluated by means of the Rayleigh dissipation function in Ref. [35]. This procedure allows the use of the generalized Lagrange or Hamilton equations. Results reported in Ref. [14] evidenced that the microscopic calculations give larger values of the viscosity coefficient than macroscopic approaches. In Ref. [36], several different macroscopic descriptions of dissipation were compared with the TDHFB approach. The modified one-body dissipation theory showed a good agreement with TDHFB results.

V. GENERALIZATION

If the blocked levels are eliminated, the system (9)–(12) reduces to

$$\begin{aligned} i\hbar\dot{\rho}_l &= \kappa_l\Delta^* - \kappa_l^*\Delta, \\ i\hbar\dot{\kappa}_l &= (2\rho_l - 1)\Delta - 2\kappa_l[\epsilon_l(t) - \lambda(t) - 2G\rho_l\kappa_l], \end{aligned} \quad (27)$$

that is, the well-known TDHFB equations [14,16]. The label m is removed from Δ_m because this quantity is now a sum over the remaining pairwise occupied levels. On the other hand, if the pairing is neglected, the third equation of the system [Eq. (11)] can be written as

$$i\hbar(\dot{c}_m c_m^* + \dot{c}_m^* c_m) = \sum_{j\neq m}^{n} h_{mj}(c_j c_m^* + c_j^* c_m). \quad (28)$$

Introducing explicitly the time dependence of the amplitudes c_m

$$c_m(t) = c_{0m}(t)\exp\left(-\frac{i}{\hbar}\int_0^t \epsilon_m(\tau)\,d\tau\right), \quad (29)$$

the next relation is obtained:

$$\begin{aligned} &i\hbar(\dot{c}_{0m}c_{0m}^* + \dot{c}_{0m}^* c_{0m}) \\ &= \sum_{j\neq m}^{n} h_{jm}\left[c_{0j}c_{0m}^*\exp\left(-\frac{i}{\hbar}\int_0^t(\epsilon_j - \epsilon_m)d\tau\right)\right. \\ &\quad \left. - c_{0j}^* c_{0m}\exp\left(\frac{i}{\hbar}\int_0^t(\epsilon_j - \epsilon_m)d\tau\right)\right]. \end{aligned} \quad (30)$$

The last relation is an equivalent form of the Landau-Zener equation (2) obtained in the framework of the single-particle model. Furthermore, if the pairing interaction is neglected, κ is zero, ρ can be either zero or unity, and the fourth equation of the system [Eq. (12)] reduces to

$$\begin{aligned} i\hbar(\dot{c}_m c_j^* + \dot{c}_j^* c_m) &= c_j^* c_m(\epsilon_m - \epsilon_j) \\ &\quad + \sum_{l\neq m,j}^{n}(h_{ml}c_j^* c_l - h_{jl}c_l^* c_m) \\ &\quad + h_{jm}(c_j^* c_j - c_m^* c_m). \end{aligned} \quad (31)$$

After introducing the exponential dependence, the next relation emerges:

$$\begin{aligned} &i\hbar(\dot{c}_{0m}c_{0j}^* + \dot{c}_{0j}^* c_{0m})\exp\left(-\frac{i}{\hbar}\int(\epsilon_m - \epsilon_j)\,d\tau\right) \\ &= \sum_{l\neq m,j}^{n}\left[h_{ml}c_{0j}^* c_{0l}\exp\left(-\frac{i}{\hbar}\int(\epsilon_l - \epsilon_j)\,d\tau\right)\right. \\ &\quad - h_{jl}c_{0l}^* c_{0m}\exp\left(-\frac{i}{\hbar}\int(\epsilon_m - \epsilon_l)\,d\tau\right)\Big] \\ &\quad + h_{mj}\left(c_{0j}^* c_{0j} - c_{0m}^* c_{0m}\right). \end{aligned} \quad (32)$$

This equation is another form of the Landau-Zener relation (2). So, the Landau-Zener equation for single-particle systems (without residual interactions) and the TDHFB equations for quasiparticles are two particular cases of the coupled-channel equations (9)–(12). So, this system represents a generalization of the TDHFB equations in the case of seniority-one nuclear systems. Similar arguments are valid also for the system (17)–(20).

VI. RESULTS

To solve the TDHFB equations, only the variations of the single-particle energies ϵ_k are needed. The simplest way to obtain the evolutions of single-particle energies is to consider a time-dependent single-particle potential in which the nucleons move independently. As evidenced in Ref. [14], such a description is within the spirit of the more rigorous Hartree-Fock approximation, which defines the potential self-consistently. However, attempts to introduce the blocking effects in the Hartree-Fock-Bogoliubov models can be found in Ref. [37].

The ^{14}C emission from ^{223}Ra will be treated. The fragments issued in this reaction are spherical while the parent is a little deformed, allowing a description in terms of a nuclear shape parametrization given by two spheres smoothly joined within a third surface.

A fine structure in the ^{14}C radioactivity of the ^{223}Ra was observed in 1989 [38–40]. In the first experiment, the results indicated that $(15 \pm 3)\%$ of ^{14}C decays are transitions on the ground state of the daughter, while $(81 \pm 6)\%$ are transitions on the first excited state. In Ref. [41], using the M3Y potential, it was evidenced that the preformation probability must be more favorable for the excited state than for the ground state with a factor of 180. Such a value cannot be accounted for by theoretical models [42] without taking into account dynamical ingredients. This is the main reason why the fine structure phenomenon was selected to validate our equations.

The deformation energy of the nuclear system is the sum between the liquid-drop energy and the shell effects, including pairing corrections [43]. The macroscopic energy is obtained in the framework of the Yukawa-plus-exponential model [44] extended for binary systems with different charge densities [45]. The Strutinsky prescriptions [46] were computed on the basis of a new version of the superasymmetric two-center shell model. This version solves a Woods-Saxon potential in terms of the two-center prescriptions as detailed in Appendix C.

Because the pairing equations diverge for an infinite number of active levels, a limited number of levels are used in the calculations: 31 levels above and 31 levels below the unpaired Fermi level in the initial ground state configuration, that is, $N - 1 = 62$. These levels are selected (in terms of the spin

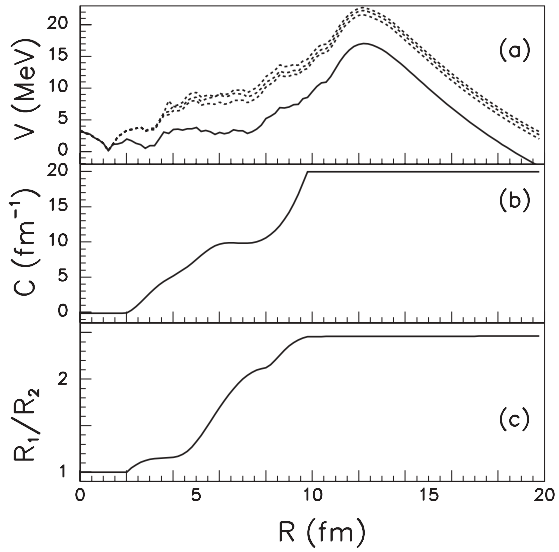

FIG. 2. (a) Deformation energy V as function of the distance between the centers of the nascent fragments R. The three excitations due to the diabatic levels ϵ_i, $i = 1, 3$ are also plotted with dotted lines. (b) Variations of the curvature of the median surface and (c) of the mass-asymmetry parameter as functions of R.

projection on the symmetry axis Ω) and kept as a single-particle energy workspace. A constant value of the pairing parameter $G = 0.13$ MeV is used.

The least action trajectory was obtained by generalizing in a three-dimensional space the method initiated in Ref. [47] and then used extensively to describe the fission processes [25–27]. The inertia is computed within the Werner-Wheeler method. The trajectory of the decaying system is obtained simultaneously as a function of three generalized coordinates, that is, the elongation R (the distance between the centers of the nascent fragments), the necking parameter $C = S/R_3$ (the curvature of the intermediate surface), and R_1/R_2 (the ratio between the radius of the heavy fragment R_1 and that of the light one R_2). These parameters are explained in Appendix C. In Fig. 2(a), the deformation energy V of the nucleus is plotted as a function of the elongation R. Three excitations of the nuclear system that correspond to the three diabatic wave functions are also plotted with dotted lines. These excitations are added to the deformation energies obtained in the framework of the macroscopic-microscopic model in order to calculate the penetrabilities as show below. In Figs. 2(b) and 2(c), the variations of the necking and mass-asymmetry generalized coordinates are displayed. At $R \approx 10$ fm, a system formed by two spherical tangent nuclei is obtained. The Woods-Saxon potential is presented in Fig. 3 for a sequence of nuclear shapes along the least action path.

To solve the time-dependent pairing equations, the single-particle level schemes for neutrons and protons must be computed along the minimal action trajectory. It is known that ^{223}Ra has the spin $\frac{3}{2}$ emerging from $1i_{11/2}$. Adiabatically, the unpaired neutron reaches the $2g_{9/2}$ level of the daughter ^{209}Pb. As also evidenced in Refs. [22,32], the fine structure in the ^{14}C radioactivity can be understood by an enhanced transition probability of the unpaired neutron from the adiabatic level $\Omega = 3/2$ emerging from $1i_{11/2}$ to the adiabatic level with the same spin projection Ω that emerges from $1j_{15/2}$, in terms of the Landau-Zener effect. The level scheme of Fig. 4

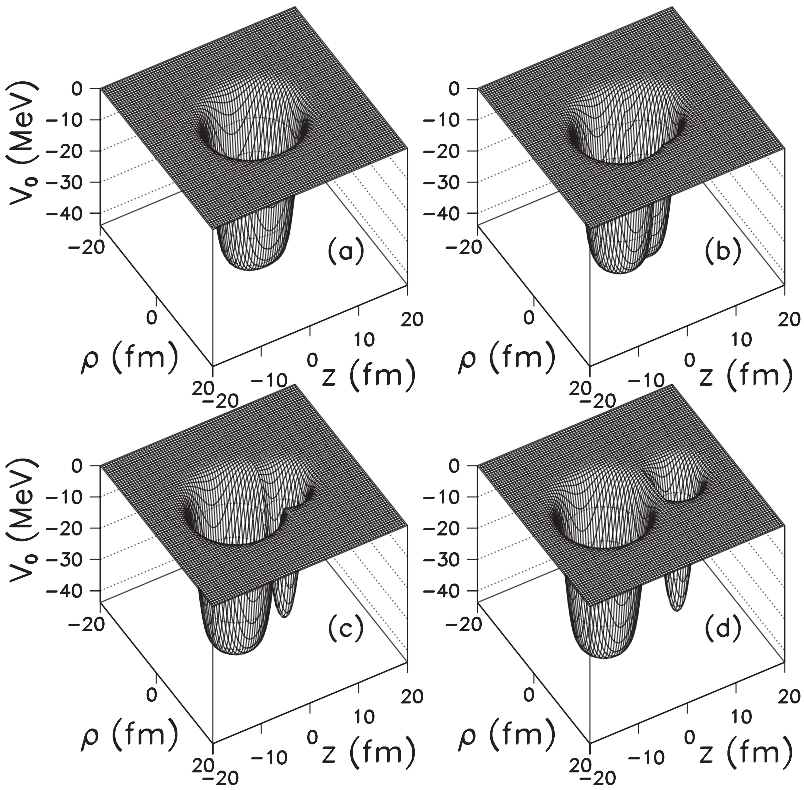

FIG. 3. Mean field Woods-Saxon potential V_0 as function of the cylindrical coordinates ρ and z for different values of the elongation R along the minimal action trajectory. (a) $R = 2$ fm, (b) $R = 5$ fm, (c) $R = 10$ fm, and (d) $R = 15$ fm.

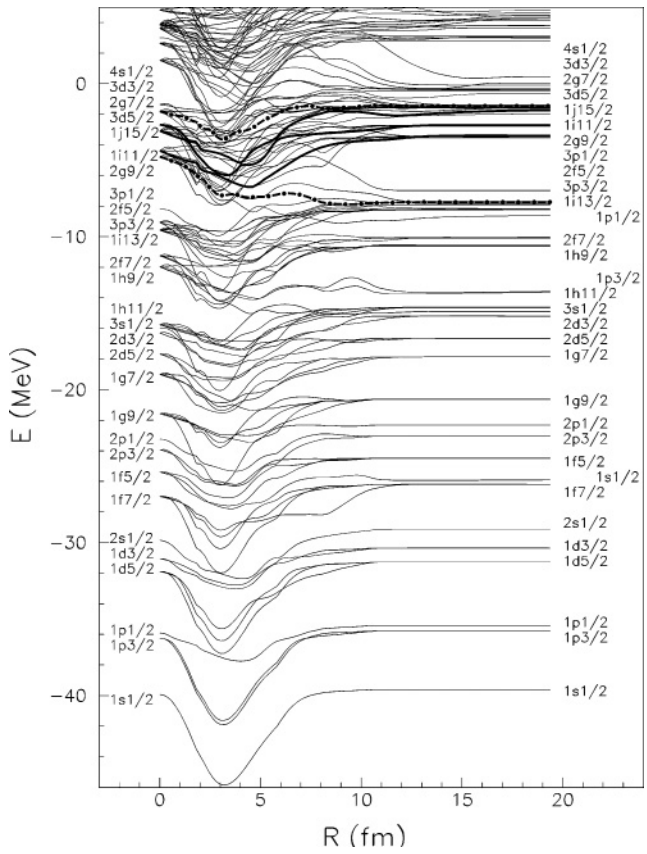

FIG. 4. Neutron energy diagram along the minimal action path as function of the distance between the centers of the fragments R. The levels with spin projection Ω of interest are plotted with thick lines. The levels are labeled with the spectroscopic factors. At the right, the first column corresponds to the daughter nucleus, while the second one is related to ^{14}C.

shows that (adiabatically) for $\Omega = 3/2$, the $1i_{11/2}$ level reaches the $2g_{9/2}$ daughter state, and the $1j_{15/2}$ level arrives on the $1i_{11/2}$ one. In this respect, the level scheme calculated within the Woods-Saxon model is in qualitative agreement with that obtained within the modified oscillator model [22]. The $\Omega = 3/2$ levels subjected to avoided level crossings that can give rise to the Landau-Zener effect are plotted with thick lines in Fig. 4. Two adjacent levels with $\Omega = 3/2$ are also plotted with point-dotted lines to show that no other avoided level crossings are possible if the unpaired neutron originates from $1i_{11/2}$. Our goal is to compute the occupation probabilities of the three levels of interest at the end of the disintegration process. For this purpose, Eqs. (18)–(20) are used. Some features concerning the less rigorous low-lying levels approach (9) and (10) can be found in Ref. [32].

In Fig. 5, the three selected diabatic levels $\epsilon_m (m = 1, 2, 3)$ are plotted together with the interaction energies h_{ij} determined by using spline interpolations around level crossings. Diabatically, the unpaired neutron, initially located on the level ϵ_1 that starts from the spherical orbital $1i_{11/2}$ will arrive on the final state $1i_{11/2}$, that is, the first single-particle excited state of the daughter, after the passage of three avoided level crossing regions.

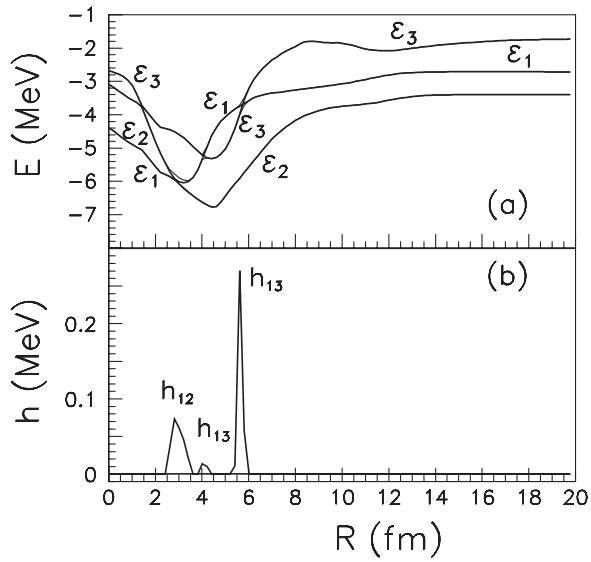

FIG. 5. (a) Selected neutron energy levels that can be occupied by a single neutron as function of the internuclear distance. Thick lines are the diabatic levels ϵ_i, $i = 1$–3, while thin lines are used for the adiabatic ones. (b) Interaction energies h_{ij} in the avoided crossing regions.

The initial conditions are determined by solving the BCS equations for the three possible seniority-one wave functions at $R \approx 1.5$ fm, where the first minimum of the deformation energy is located. The time-dependent pairing equations are integrated numerically using the Runge-Kutta method. The occupation probabilities p_m and the dissipated energies given by formula (23) are determined along the minimal action path for an internuclear velocity $\frac{\partial R}{\partial t} = 1.4 \times 10^6$ m/s. This value can be translated in a time required to penetrate the barrier of about 1.4×10^{-20} s.

In Fig. 6, the probability of occupations p_m with an unpaired neutron of the three diabatic levels are presented as a function of the internuclear distance. In the bottom panel, the three dissipated energies ΔE_m and the energy dissipated in the proton level scheme are also displayed. For comparison, the occupation probabilities calculated with the Landau-Zener formula (2) are displayed with the dashed line in panels (a)–(c). It can be noticed that the occupation probabilities of the diabatic levels have a more pronounced variation in the avoided crossing region when the residual pairing correlation is neglected.

The branching ratio r between the partial half-life for transitions to the ground state of the daughter and the partial half-live to the first excited state is given by

$$r = \frac{p_1 \exp(-K_1)}{p_2 \exp(-K_2)}, \tag{33}$$

where the index corresponds to the diabatic level ϵ_1 or ϵ_2, and

$$K_m = \frac{2}{\hbar} \int_{R_{\text{g.s.}}}^{R_m} \sqrt{2\mu[V(R) + D_m(R) - V(R_{\text{g.s.}})]}\, dR \tag{34}$$

are the WKB integrals. Here $R_{\text{g.s.}}$ is the ground state elongation, R_m is the exit point from the barrier for the channel m, $V(R)$ is the macroscopic-microscopic energy,

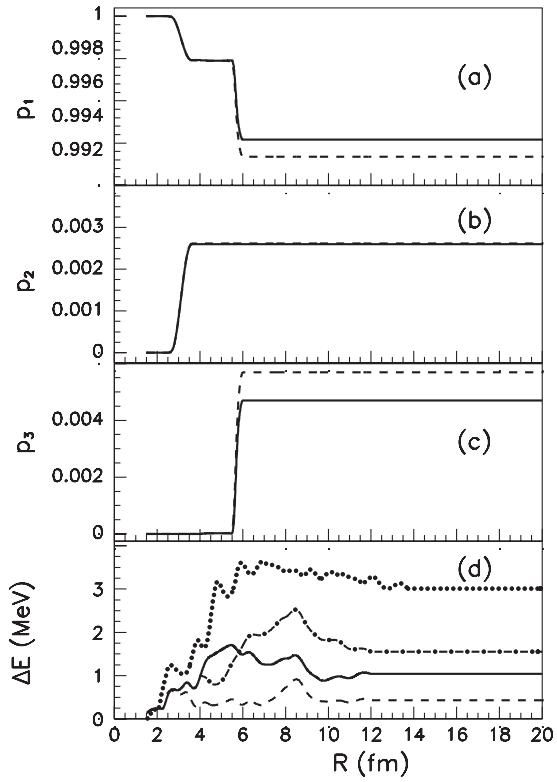

FIG. 6. (a) Full line: occupation probability p_1 of the diabatic level ϵ_1 as function of the internuclear distance R. Dashed line: occupation probability p_1 computed without residual interactions. (b) Occupation probability p_2 of ϵ_2. (c) Occupation probability p_3 of ϵ_3. (d) Dissipated energies. Solid line: ΔE_1 for ϵ_1. Dashed line: ΔE_2 for ϵ_2. Dot-dashed line: ΔE_3 for ϵ_3. Dotted line: ΔE_p due to the proton level scheme.

$D_m(R) = \Delta E_m(R) + \Delta E_p(R)$ is the dissipated energy with ΔE_m being the specialization energy given by Eq. (23) and ΔE_p denoting the dissipated energy of the proton subsystem, and μ is the reduced mass. ΔE_p is calculated with Eq. (27). The barriers obtained for $V(R) + D_m(R)$ are plotted in Fig. 2(a) with dotted lines. The experimental values of r range between 5.4 and 5.9. Our theoretical value is $r = 5.48$, which is in excellent agreement with experimental data.

Evidence of Landau-Zener diabatic transitions signature has been observed in nuclear collision and disintegration processes such as fusion [48], inelastic scattering [20,21,49–51], α and cluster decay [22–24], and fission [25–27]. In these works, some equivalent forms of Landau-Zener equation (2) were used, without taking into account the residual interaction. The new equations (9)–(12) and (17)–(20) allow one to consider the effect of pairing. As it can be inferred from Ref. [52], the major part of mean field dynamical investigations involves the time-dependent Hartree-Fock theory, and only a few TDHFB calculations have been performed up to now, as, for example, in Refs. [14–17,36,53–56]. Usually, only reactions involving even-even systems are reported. Extended TDHB equations have been derived from the semiclassical transport equations in Refs. [57,58] or from the classical Euler-Lagrange formalism in Ref. [59]. These equations are applicable to odd fermion systems but do not take into account the Landau-Zener effect. For the first time, the formalism presented in this work offers a way to treat the evolution in time and the dynamical excitations of an unpaired single particle.

In the present work, the time-dependent equations are derived by involving the variational principle in a way similar to that of Ref. [16]. Alternatively, in Ref. [14] the system (27) is obtained from the Heisenberg form of the equations of motion. In the treatment of Ref. [14], a full solution of the dynamics describing the time evolution emerges. This full solution reflects more accurately the response of the nuclear system to the changing single-particle potential. The system (27) is only a particular form of the full solution. This particular form is obtained by neglecting the antisymmetric time-derivative matrix of the wave functions. Using this approximation, it is believed that the major part of the collective energy associated with the coherent movement of the nucleons is eliminated.

In conclusion, two approaches that generalize the Landau-Zener equations for seniority-one superfluid systems are presented. The new formalism is valid for any kind of mean field approximation that includes a monopole pairing field. The equations that describe our approaches offer information about the spectroscopic amplitudes and the dissipated energies in different final channels. The new equations were used to reproduce the qualitative and quantitative features of the fine structure phenomenon in cluster decay. Up to now, this phenomenon was not described adequately in the framework of models that do not include dynamical ingredients, as evidenced in Ref. [60]. Within the time-dependent pairing equations, a good agreement with experimental data was obtained. A new version of the superasymmetric two-center shell model based on a Woods-Saxon potential was developed and used in this context. The model can be further improved to take into consideration the Coriolis coupling in a way evidenced previously in Ref. [24] to investigate fine structure due to rotational states [61,62].

ACKNOWLEDGMENTS

The author thanks D. S. Delion and D. Mihalache for reading the manuscript and making constructive comments. This work was partially supported within the framework of the IDEI program of the Romanian Ministry of Education and Research.

APPENDIX A

The TDHFB equations in which the blocking effect is neglected will be derived in this Appendix. Following the same prescriptions as in Ref. [16] and using the time-dependent Hamiltonian of Eq. (6) within the corrections in Eq. (7), and the trial wave functions of Eq. (5), the expected value of the energy functional is obtained:

$$\langle\varphi|H - i\hbar\frac{\partial}{\partial t} + H' - \lambda N|\varphi\rangle = \sum_m^n |c_m|^2 \left\{ 2\sum_{k\neq m} |v_k|^2(\epsilon_k - \lambda) + (\epsilon_m - \lambda) \right.$$

$$- G \left| \sum_{k\neq m} u_k^* v_k \right|^2 - G \sum_{k\neq m} |v_k|^4 | \Bigg\}$$
$$- i\hbar \sum_m^n |c_m|^2 \left[\sum_{k\neq m} \frac{1}{2} (v_k^* \dot{v}_k - \dot{v}_k^* v_k) \right]$$
$$- i\hbar \sum_m^n c_m^* \dot{c}_m + \sum_{m,j\neq m}^n h_{mj} c_m^* c_j . \tag{A1}$$

The following identities were used:

$$\langle \varphi | \sum_k \epsilon_k (a_k^+ a_k + a_{\bar{k}}^+ a_{\bar{k}}) | \varphi \rangle = \sum_m^n |c_m|^2 \left[\epsilon_m + 2 \sum_{k\neq m} \epsilon_k |v_k|^2 \right], \tag{A2}$$

$$\langle \varphi | \sum_{kl} a_k^+ a_{\bar{k}}^+ a_l a_{\bar{l}} | \varphi \rangle = \sum_m^n |c_m|^2 \left(\sum_{k\neq m} |v_k|^4 + \sum_{l\neq m} u_l v_l^* \sum_{k\neq m} u_k v_k \right), \tag{A3}$$

$$\langle \varphi | \alpha_i^+ \alpha_j + \alpha_j^+ \alpha_i | \varphi \rangle = c_i^* c_j + c_j^* c_i , \tag{A4}$$

and

$$\langle \varphi | \frac{\partial}{\partial t} | \varphi \rangle = \sum_m^n \left[c_m^* \dot{c}_m + |c_m|^2 \sum_{k\neq m} (u_k \dot{u}_k + v_k^* \dot{v}_k) \right], \tag{A5}$$

because, as evidenced in Ref. [16],

$$\int (\phi_k^* \dot{\phi}_k + \dot{\phi}_k^* \phi_k) d^3 r = 0, \tag{A6}$$

where $|\phi_k\rangle = a_k^+ |0\rangle$, due to the normalization. The equality $\dot{u}_k = -(\dot{v}_k^* v_k + \dot{v}_k v_k^*)/(2u_k)$ is also used.

To minimize the functional, the expression (A1) is derived with respect to the independent variables v_l and v_l^*. Two equations follow:

$$\sum_m^n |c_m|^2 \left\{ 2v_l^* (\epsilon_l - \lambda) - G \left[\sum_{k\neq m} \kappa_k \left(-\frac{v_l^* v_l^*}{2u_l} \right) + \left(u_l - \frac{\rho_l}{2u_l} \right) \sum_{k\neq m} \kappa_k^* + 2\rho_l v_l^* \right] + i\hbar \dot{v}_l^* \right\} = 0, \tag{A7}$$

and its complex conjugate. Here the notations for densities $\rho = |v|^2$ and pairing moment components $\kappa = uv$ are introduced. To derive the previous expression, the next relation is also used:

$$\frac{\partial u_k}{\partial v_k^*} = \frac{\partial \sqrt{1 - |v_k|^2}}{\partial v_k^*} = -\frac{1}{2\sqrt{1 - |v_k|^2}} \frac{\partial (v_k v_k^*)}{\partial v_k^*} = -\frac{v_k}{2u_k}. \tag{A8}$$

As mentioned previously, u_k is a real quantity and v_k a complex one.

The condition of conservation of the number of particles

$$2 \sum_k |v_k|^2 = N + 2\rho_F - 1 \tag{A9}$$

was used so that

$$\sum_k (\dot{v}_k^* v_k + v_k^* \dot{v}_k) = 0, \tag{A10}$$

$$\frac{\partial}{\partial v_k} (\dot{v}_k^* v_k + v_k^* \dot{v}_k) = 0, \tag{A11}$$

and

$$\frac{\partial}{\partial v_k} v_k^* \dot{v}_k = -\dot{v}_k^* . \tag{A12}$$

Multiplying Eq. (A7) and its complex conjugate with v_l^* and v_l, respectively, and subtracting, the first TDHFB equation (9) is obtained:

$$i\hbar \dot{\rho}_l = \frac{\sum_m^n |c_m|^2 \{\kappa_l \Delta_m^* - \kappa_l^* \Delta_m\}}{\sum_m^n |c_m|^2}, \tag{A13}$$

where $\sum_m |c_m|^2 = 1$ and $\Delta_m = G \sum_{k\neq m} \kappa_k$.

Another equation can be obtained:

$$\dot{\kappa}_l = -\frac{v_l}{2u_l} \dot{\rho}_l + u_l \dot{v}_l = -\frac{v_l}{2u_l} \frac{1}{i\hbar} \sum_m^n |c_m|^2 \times \{\kappa_l \Delta_m^* - \kappa_l^* \Delta_m\} + \frac{u_l}{i\hbar} \sum_m^n |c_m|^2 \times \left[2v_l (\epsilon_l - \lambda) - \Delta_m^* \left(-\frac{v_l v_l}{2u_l} \right) - \left(u_l - \frac{\rho_l}{2u_l} \right) \Delta_m - 2G\rho_l v_l \right], \tag{A14}$$

so that the second TDHFB equation (10) follows:

$$i\hbar \dot{\kappa}_l = \sum_m^n |c_m|^2 \left\{ (2\rho_l - 1) \Delta_m + 2\kappa_l (\epsilon_l - \lambda) - 2G\rho_l \kappa_l \right\}. \tag{A15}$$

Using the property

$$\sum_m^n |c_m|^2 = 1, \tag{A16}$$

so that

$$\sum_m^n \dot{c}_m c_m^* = -\sum_m^n \dot{c}_m^* c_m , \tag{A17}$$

Eq. (A1) is derived with respect to c_m and c_m^* and set to zero. Two relations are obtained:

$$- i\hbar \dot{c}_m^* = c_m^* \left[2 \sum_{k\neq m} |v_k|^2 (\epsilon_k - \lambda) + (\epsilon_m - \lambda) - G \left| \sum_{k\neq m} u_k^* v_k \right|^2 - G \sum_{k\neq m} |v_k|^4 \right]$$

$$-i\hbar c_m^* \left[\sum_{k\neq m}\frac{1}{2}(v_k^*\dot{v}_k - \dot{v}_k^* v_k)\right] + \sum_{j\neq m}^{n} h_{mj}c_j^*, \tag{A18}$$

and its complex conjugate.

Equations (A13), (A15), and (A18) contain all the information on the dynamics. Multiplying the relation (A18) and its complex conjugate with c_m and c_m^* and subtracting them, the next relation follows:

$$i\hbar(\dot{c}_m c_m^* + \dot{c}_m^* c_m) = \sum_{j\neq m}^{n} h_{mj}(c_j c_m^* - c_j^* c_m). \tag{A19}$$

It is a form of the third TDHFB equation [Eq. (11)]. For a passage through only one avoided crossing region (m, j), only two amplitudes, c_m and c_j, can change. On the other hand, from the conservation condition one obtains

$$\dot{c}_m c_m^* + c_m \dot{c}_m^* = -(\dot{c}_j c_j^* + c_j \dot{c}_j^*). \tag{A20}$$

This condition is fulfilled by the Eq. (A19), so that the equation conserves the norm. Changing indexes, multiplying with amplitudes, and subtracting relation (A18) and its complex conjugate, the next equation follows:

$$\begin{aligned} &i\hbar(\dot{c}_m c_j^* + \dot{c}_j^* c_m) \\ &= c_m c_j^* \left\{-\frac{1}{G}(|\Delta_m|^2 - |\Delta_j|^2) + 2\,|v_j|^2(\epsilon_j - \lambda) + (\epsilon_m - \lambda)\right. \\ &\quad \left. - G\rho_j^2 - 2|\,v_m|^2(\epsilon_m - \lambda) - (\epsilon_j - \lambda) + G\rho_m^2\right\} \\ &\quad + c_m c_j^* \frac{i\hbar}{2}(v_m^*\dot{v}_m^* - \dot{v}_m^* v_m - v_j^*\dot{v}_j + \dot{v}_j^* v_j) \\ &\quad + \sum_{l\neq m}^{n} h_{lm}c_l c_j^* - \sum_{l\neq j}^{n} h_{lj}c_l^* c_m. \end{aligned} \tag{A21}$$

From Eqs. (A7) and its complex conjugate, the expressions in the last parenthesis that involve $\dot{v}$ and $\dot{v}^*$ can be obtained:

$$\begin{aligned} \frac{i\hbar}{2}(v_l^*\dot{v}_l - \dot{v}_l^* v_l) &= 2\rho_l(\epsilon_l - \lambda) + \frac{\sum_m^n p_m\Delta_m}{2}\left(\frac{\rho_l^2}{\kappa_l} - \kappa_l^*\right) \\ &\quad + \frac{\sum_m^n p_m\Delta_m^*}{2}\left(\frac{\rho_l^2}{\kappa_l^*} - \kappa_l\right) - 2G\rho_l^2. \end{aligned} \tag{A22}$$

Using the notations in Eq. (13) and rearranging the terms, the fourth TDHFB equation [Eq. (12)] is eventually obtained.

APPENDIX B

The TDHFB equations in which the blocking effect is taken into consideration are derived in this Appendix. Using the corrections in Eq. (15) and the trial wave functions in Eq. (14), the expected value of the Lagrange function is

$$\begin{aligned} &\langle\varphi|H - i\hbar\frac{\partial}{\partial t} + H' - \lambda N|\varphi\rangle \\ &= \sum_m^n |c_m|^2 \left\{2\sum_{k\neq m}|v_{k(m)}|^2(\epsilon_k - \lambda_m) + (\epsilon_m - \lambda_m)\right. \\ &\quad \left. - G\left|\sum_{k\neq m} u_{k(m)}v_{k(m)}\right|^2 - G\sum_{k\neq m}|v_{k(m)}|^4\right\} \\ &\quad - i\hbar\sum_m^n |c_m|^2\left[\sum_{k\neq m}\frac{1}{2}(v_{k(m)}^*\dot{v}_{k(m)} - \dot{v}_{k(m)}^* v_{k(m)})\right] \\ &\quad - i\hbar\sum_m^n c_m^*\dot{c}_m + \sum_{m,j\neq m}^{n} h_{mj}c_m^* c_j. \end{aligned} \tag{B1}$$

To minimize the functional, expression (B1) is derived with respect to the independent variables $v_{l(m)}$ and $v_{l(m)}^*$ by taking into account the subsidiary condition (A12). Two relations follow:

$$\begin{aligned} &\sum_m^n |c_m|^2 \left\{2v_{l(m)}^*(\epsilon_l - \lambda_m) - G\left[\sum_{k\neq m}\kappa_{k(m)}\left(-\frac{v_{l(m)}^* v_{l(m)}^*}{2u_{l(m)}}\right)\right.\right. \\ &\quad \left.\left. + \left(u_{l(m)} - \frac{\rho_{l(m)}}{2u_{l(m)}}\right)\sum_{k\neq m}\kappa_{k(m)}^* + 2\rho_{l(m)}v_{l(m)}^*\right] \right. \\ &\quad \left. + i\hbar\dot{v}_{l(m)}^*\right\} = 0, \end{aligned} \tag{B2}$$

and its complex conjugate. This system can be solved by considering that the expression in the curly bracket is zero for each value of m. Following a similar approach as in Appendix A, the first two TDHFB equations associated with an unpaired nucleon in the state m emerge:

$$i\hbar\dot{\rho}_{l(m)} = \kappa_{l(m)}\Delta_m^* - \kappa_{l(m)}^*\Delta_m, \tag{B3}$$

$$\begin{aligned} i\hbar\dot{\kappa}_{l(m)} &= \left(2\rho_{l(m)} - 1\right)\Delta_m + 2\kappa_{l(m)}(\epsilon_l - \lambda_m) \\ &\quad - 2G\rho_{l(m)}\kappa_{l(m)}. \end{aligned} \tag{B4}$$

To obtain the probability that an unpaired nucleon is located on a state m, the expression (B1) must be derived with respect to c_m and c_m^*. Two equations follow:

$$\begin{aligned} -i\hbar\dot{c}_m^* &= c_m^*\left[2\sum_{k\neq m}|v_{k(m)}|^2(\epsilon_k - \lambda_m) + \epsilon_m - \lambda_m\right. \\ &\quad - G\left|\sum_{k\neq m}u_{k(m)}v_{k(m)}\right|^2 - G\sum_{k\neq m}|v_{k(m)}|^4 \\ &\quad \left. - i\hbar c_m^*\sum_{k\neq m}\frac{1}{2}(v_{k(m)}^*\dot{v}_{k(m)} - \dot{v}_{k(m)}^* v_{k(m)})\right] \\ &\quad + \sum_{j\neq m}^{n} h_{mj}c_j^* = 0, \end{aligned} \tag{B5}$$

and its complex conjugate. Multiplying Eq. (B5) with c_m, its complex conjugates with c_m^*, and subtracting, we obtain

$$i\hbar(\dot{c}_m c_m^* + \dot{c}_m^* c_m) = \sum_{j\neq m}^{n} h_{mj}(c_j c_m^* - c_j^* c_m). \tag{B6}$$

Using the notations in Eq. (13), then Eq. (19) follows.

From relations (B5) and its complex conjugate, another relation can be deduced:

$$\begin{aligned}
&i\hbar(\dot{c}_j^* c_m + \dot{c}_m c_j^*) \\
&= c_m c_j^* \Bigg[-\frac{1}{G}(|\Delta_m|^2 - |\Delta_j|^2) + (\epsilon_m - \epsilon_j - \lambda_m + \lambda_j) \\
&\quad + 2\sum_{k\neq m} \rho_{k(m)}(\epsilon_k - \lambda_m) - 2\sum_{k\neq j} \rho_{k(j)}(\epsilon_k - \lambda_j) \\
&\quad - G\left(\sum_{k\neq m} \rho_{k(m)}^2 - \sum_{k\neq j} \rho_{k(j)}^2\right)\Bigg] \\
&\quad - \frac{i\hbar}{2} c_m \dot{c}_j^* \Bigg[\sum_{k\neq m}(v_{k(m)}^* \dot{v}_{k(m)} - \dot{v}_{k(m)}^* v_{k(m)}) \\
&\quad - \sum_{k\neq j}(v_{k(j)}^* \dot{v}_{k(j)} - \dot{v}_{k(j)}^* v_{k(j)})\Bigg] \\
&\quad + \sum_{l\neq m}^{n} h_{lm} c_l c_j^* - \sum_{l\neq j}^{n} h_{lj} c_l^* c_m.
\end{aligned} \tag{B7}$$

The derivatives $\dot{v}$ and $\dot{v}^*$ appear in the previous expression. To evaluate quantities in which these derivatives intervene, Eq. (B2) and its complex conjugate are used. The next relation follows:

$$\begin{aligned}
&\frac{i\hbar}{2}(v_{l(m)}^* \dot{v}_{l(m)} - \dot{v}_{l(m)}^* v_{l(m)}) \\
&= \frac{v_{l(m)}^*}{2}\Bigg\{(2v_{l(m)}(\epsilon_l - \lambda_m) \\
&\quad - G\Bigg[\sum_{k\neq m} \kappa_{k(m)}^* \left(-\frac{v_{l(m)}^* v_{l(m)} v_{l(m)}}{2v_{l(m)}^* u_{l(m)}} + \left(u_{l(m)} - \frac{\rho_{l(m)}}{2u_{l(m)}}\right)\right) \\
&\quad \times \sum_{k\neq m} \kappa_{k(m)} + 2\rho_{l(m)} v_{l(m)}\Bigg]\Bigg\} + \frac{v_{l(m)}}{2}\Bigg\{(2v_{l(m)}^*(\epsilon_l - \lambda_m) \\
&\quad - G\Bigg[\sum_{k\neq m} \kappa_{k(m)} \left(-\frac{v_{l(m)} v_{l(m)}^* v_{l(m)}^*}{2v_{l(m)} u_{l(m)}} + \left(u_{l(m)} - \frac{\rho_{l(m)}}{2u_{l(m)}}\right)\right) \\
&\quad \times \sum_{k\neq m} \kappa_{k(m)}^* + 2\rho_{l(m)} v_{l(m)}^*\Bigg]\Bigg\} \\
&= \rho_{l(m)}(\epsilon_l - \lambda_m) + \frac{\Delta_m^*}{2}\frac{\rho_{l(m)}^2}{2\kappa_{l(m)}^*} \\
&\quad - \left(\kappa_{l(m)}^* - \frac{\rho_{l(m)}^2}{2\kappa_{l(m)}}\right)\frac{\Delta_m}{2} - G\rho_{l(m)}^2 + \rho_{l(m)}(\epsilon_l - \lambda_m) \\
&\quad + \frac{\Delta_m}{2}\frac{\rho_{l(m)}^2}{2\kappa_{l(m)}} - \left(\kappa_{l(m)} - \frac{\rho_{l(m)}^2}{2\kappa_{l(m)}^*}\right)\frac{\Delta_m^*}{2} - G\rho_{l(m)}^2 \\
&= 2\rho_{l(m)}(\epsilon_l - \lambda_m) - 2G\rho_{l(m)}^2 + \frac{\Delta_m^*}{2}\left(\frac{\rho_{l(m)}^2}{\kappa_{l(m)}^*} - \kappa_{l(m)}\right) \\
&\quad + \frac{\Delta_m}{2}\left(\frac{\rho_{l(m)}^2}{\kappa_{l(m)}} - \kappa_{l(m)}^*\right),
\end{aligned} \tag{B8}$$

so that relation (B7) becomes

$$\begin{aligned}
&i\hbar\dot{S}_{jm} \\
&= c_m c_j^*\Bigg\{-\frac{1}{G}\left(|\Delta_m|^2 - |\Delta_j|^2\right) + (\epsilon_m - \epsilon_j - \lambda_m + \lambda_j) \\
&\quad + G\left(\sum_{k\neq m} \rho_{k(m)}^2 - \sum_{k\neq j} \rho_{k(j)}^2\right) \\
&\quad - \frac{1}{2}\sum_{k\neq m}\left[\Delta_m\left(\frac{\rho_{k(m)}^2}{\kappa_{k(m)}} - \kappa_{k(m)}^*\right) + \Delta_m^*\left(\frac{\rho_{k(m)}^2}{\kappa_{k(m)}^*} - \kappa_{k(m)}\right)\right] \\
&\quad + \frac{1}{2}\sum_{k\neq j}\left[\Delta_j\left(\frac{\rho_{k(j)}^2}{\kappa_{k(j)}} - \kappa_{k(j)}^*\right) + \Delta_j^*\left(\frac{\rho_{k(j)}^2}{\kappa_{k(j)}^*} - \kappa_{k(j)}\right)\right]\Bigg\} \\
&\quad + \sum_{k\neq j,m}^{n} h_{mk} c_k c_j^* - \sum_{k\neq j,m}^{n} h_{kj} c_k^* c_m + h_{mj} c_j c_j^* - h_{jm} c_m^* c_m.
\end{aligned} \tag{B9}$$

After some rearrangement of terms and using Eq. (13), Eq. (20) is eventually obtained.

APPENDIX C

A two-center shell model with a Woods-Saxon potential was developed recently [63]. An axial symmetric nuclear shape parametrization is used to determine the mean field potential. This nuclear shape parametrization is given by two ellipsoids (of different semiaxes and eccentricities) smoothly joined with a third surface given by the rotation of a circle around the axis of symmetry as displayed in Fig. 7. The parametrization is characterized by five degrees of freedom that can be associated, for example, to the elongation ($R = z_2 - z_1$), to the necking ($C = S/R_3$), to the mass asymmetry ($\eta = a_1/a_2$), and to the deformations of the two fragments ($b_i/a_i, i = 1, 2$). Treating the ^{14}C emission, the deformations of the two fragments can be neglected, and the mass asymmetry parameter is considered as $\eta = R_1/R_2$. The mean field potential is defined in the frame

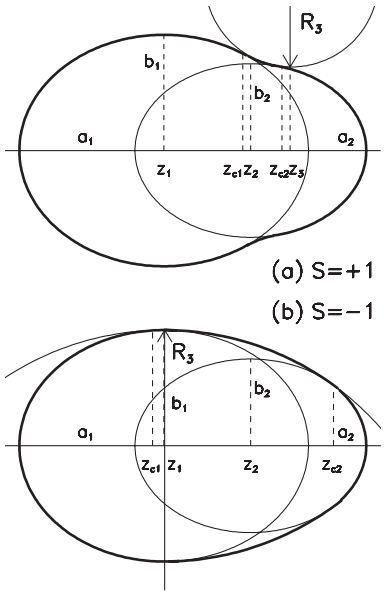

FIG. 7. Nuclear shape parametrization. Two intersected ellipsoids of different eccentricities are smoothly joined with a third surface. Two cases can be obtained: (a) the curvature of the circle of radius R_3 is positive ($s = 1$), and (b) the curvature of R_3 is negative ($s = -1$). The elongation is given by the distance between the centers of the ellipsoids, $R = z_2 - z_1$.

of the Woods-Saxon model as

$$V_0(\rho, z) = -\frac{V_c}{1 + \exp\left[\frac{\Delta(\rho,z)}{a}\right]} \tag{C1}$$

where $\Delta(\rho, z)$ represents the distance between a point (ρ, z) and the nuclear surface. This distance is measured only along the normal direction on the surface, and it is negative if the point (ρ, z) is located in the interior of the nucleus. V_c is the depth of the potential, while a is the diffuseness parameter. In our work, the depth is $V_c = V_{0c}[1 \pm \kappa(N_0 - Z_0)/N_0 + Z_0)]$ with plus sign for protons and minus sign for neutrons, $V_{0c} = 51$ MeV, $a = 0.67$ fm, $\kappa = 0.67$. Here A_0, N_0, and Z_0 represent the mass number, neutron number ,and charge number of the parent, respectively. This parametrization, referred to as the Blomqvist-Wahlborn one in Ref. [64], is adopted because it provides the same radius constant r_0 for the mean field and the pairing field. That ensures a consistency of the shapes of the two fields at hyperdeformations, i.e., two tangent ellipsoids.

In Fig. 3, the mean field potential V_0 is plotted as a function of cylindrical coordinates ρ and z for four nuclear shape configurations obtained along the minimal action path. The spin-orbit coupling is assumed to have the form

$$V_{ls} = -2\lambda\left(\frac{1}{2mc}\right)^2 (\nabla V_0 \times \vec{p})\vec{s}, \tag{C2}$$

where $\lambda = 35$ is a dimensionless coupling constant and m is the nucleon mass, while c denotes the speed of light. The spherical components of the operator

$$L = \nabla V \times p \tag{C3}$$

in cylindrical coordinates are

$$L^{\pm} = \mp\hbar\, e^{\pm i\varphi}\left(\frac{\partial V_0}{\partial\rho}\frac{\partial}{\partial z} - \frac{\partial V_0}{\partial z}\frac{\partial}{\partial\rho} \pm i\frac{\partial V_0}{\partial z}\frac{1}{\rho}\frac{\partial}{\partial\varphi}\right), \tag{C4}$$

$$L_z = i\hbar\frac{\partial V_0}{\partial\rho}\frac{1}{\rho}\frac{\partial}{\partial\varphi}, \tag{C5}$$

so that

$$Ls = \tfrac{1}{2}(L^+ s^- + L^- s^+) + L_z s_z \tag{C6}$$

The next step is to obtain the solutions of the Schrödinger equation

$$\left[-\frac{\hbar^2}{2m}\Delta + V_0(\rho, z) + V_{ls}(\rho, z) + V_C(\rho, z)\right]\Psi(\rho, z, \varphi) = E\Psi(\rho, z, \varphi). \tag{C7}$$

For protons, a Coulomb term V_C is added, as in Refs. [64,65]. No analytical solutions can be found for such potentials. A suitable eigenvector basis able to diagonalize the Woods-Saxon potential can be obtained within the double-center harmonic oscillator model.

A complete analytical eigenvector basis can only be obtained for the semisymmetric two-center oscillator. This potential corresponds to a shape parametrization given by two ellipsoids that possess the same semiaxis perpendicular on the axis of symmetry. The potential is

$$V_o(\rho, z) = \begin{cases} \frac{1}{2}m\omega_{z1}^2(z - c_1)^2 + \frac{1}{2}m\omega_\rho^2, & z < 0, \\ \frac{1}{2}m\omega_{z2}^2(z - c_2)^2 + \frac{1}{2}m\omega_\rho^2, & z \geqslant 0, \end{cases} \tag{C8}$$

where ω denotes the stiffness of the potential along different directions, that is, $\omega_{z1} = \omega_0\frac{R_0}{a_1}$, $\omega_{z2} = \omega_0\frac{R_0}{a_2}$, and $\omega_\rho = \omega_0\frac{R_0}{b_1}$, with $\omega_0 = 41A_0^{-1/3}$ and $R_0 = r_0A_0^{1/3}$, in order to ensure a constant value of the potential on the surface. The origin on the z axis is considered to be the location of the plane of intersection between the two ellipsoids.

An analytic system of eigenvectors can be obtained for V_0 by solving the Schrödinger equation:

$$\left[-\frac{\hbar^2}{2m_0}\Delta + V_o(\rho, z)\right]\Psi(\rho, z, \varphi) = E\Psi(\rho, z, \varphi). \tag{C9}$$

The analytic solution of Eq. (C9) is obtained using the ansatz

$$\Psi(\rho, z, \varphi) = Z(z)R(\rho)\Phi(\varphi), \tag{C10}$$

with

$$\Phi_m(\varphi) = \frac{1}{\sqrt{2\pi}}\exp(im\varphi), \tag{C11}$$

$$R_{nm}(\rho) = \sqrt{\frac{2n!}{(n+m)!}}\alpha_\rho \exp\left(-\frac{\alpha_\rho^2\rho^2}{2}\right)(\alpha_\rho\rho)^m L_n^m\left(\alpha_\rho^2\rho^2\right), \tag{C12}$$

$$Z_\nu(z) = \begin{cases} C_{\nu_1}\exp\left(-\frac{\alpha_{z1}^2(z-c_1)^2}{2}\right)\mathbf{H}_{\nu_1}[-\alpha_{z1}(z + c_1)], \\ z < 0, \\ C_{\nu_2}\exp\left(-\frac{\alpha_{z2}^2(z-c_2)^2}{2}\right)\mathbf{H}_{\nu_2}[\alpha_{z2}(z - c_2)], \\ z \geqslant 0, \end{cases} \tag{C13}$$

where $L_n^m(x)$ is the Laguerre polynomial, $\mathbf{H}_\nu(\zeta)$ is the Hermite function, $\alpha_i = (m_0\omega_i/\hbar)^{1/2} (i = z1, z2, \rho)$ are length parameters, and C_{ν_i} denotes the normalization constants. The quantum numbers n and m are integers, while the quantum number ν along the z axis is real and has different values for the intervals $(-\infty, 0]$ and $[0, \infty)$. Imposing conditions for the continuity of the wave function and its derivative, together with those for the stationary energy and orthonormality, the values of ν_1, ν_2, C_{ν_1}, and C_{ν_2} are obtained. Details concerning these solutions and expressions for the normalization constants can be found in Refs. [66,67]. For reflection-symmetric shapes, the solutions along the z axis are also characterized by the parity as a good quantum number. The basis [Eq. (C13)] for the two-center oscillators can be used for various ranges of models which are more or less phenomenological ones [68,69]. On the other hand, there are different ways to obtain the single-particle energies for a two-center Woods-Saxon potential. Other recipes are given in Ref. [70] where the potentials are expanded in terms of harmonic oscillator functions.

[1] C. Simenel and B. Avez, Int. J. Mod. Phys. E **17**, 31 (2008).
[2] T. Nakatsukasa and K. Yabana, Phys. Rev. C **71**, 024301 (2005).
[3] A. S. Umar and V. E. Oberacker, Phys. Rev. C **71**, 034314 (2005).
[4] J. A. Maruhn, P. G. Reinhard, P. D. Stevenson, J. R. Stone, and M. R. Strayer, Phys. Rev. C **71**, 064328 (2005).
[5] J. Rikovska Stone, J. Phys. G **31**, R211 (2005).
[6] D. L. Hill and J. A. Wheeler, Phys. Rev. **89**, 1102 (1953).
[7] H. Goutte, J. F. Berger, P. Casoli, and D. Gogny, Phys. Rev. C **71**, 024316 (2005).
[8] J. F. Berger, M. Girod, and D. Gogny, Nucl. Phys. **A428**, 23c (1984).
[9] C.-Y. Wong and H. H. K. Tang, Phys. Rev. C **20**, 1419 (1979).
[10] P. Grange, J. Richert, G. Wolschin, and H. A. Weidenmuller, Nucl. Phys. **A356**, 260 (1981).
[11] G. Mantzouranis and H.-C. Pauli, Phys. Rev. C **22**, 1550 (1980).
[12] Y. Abe, S. Ayik, P.-G. Reinhard, and E. Suraud, Phys. Rep. **275**, 49 (1996).
[13] D. Lacroix, S. Ayik, and Ph. Chomaz, Prog. Part. Nucl. Phys. **52**, 497 (2004).
[14] S. E. Koonin and J. R. Nix, Phys. Rev. C **13**, 209 (1976).
[15] G. Schütte and L. Wilets, Z. Phys. A **286**, 313 (1978).
[16] J. Blocki and H. Flocard, Nucl. Phys. **A273**, 45 (1976).
[17] M. Mirea, L. Tassan-Got, C. Stephan, and C. O. Bacri, Nucl. Phys. **A735**, 21 (2004).
[18] B. Avez, C. Simenel, and Ph. Chomaz, Phys Rev. C (to be published), arXiv:0808.3507v1 [nucl-th].
[19] Y. Hasimoto and K. Nokedi, arXiv:0707.3083v1 [nucl-th].
[20] M. H. Cha, J. Y. Park, and W. Scheid, Phys. Rev. C **36**, 2341 (1987).
[21] J. Y. Park, W. Greiner, and W. Scheid, Phys. Rev. C **21**, 958 (1980).
[22] M. Mirea, Phys. Rev. C **57**, 2484 (1998).
[23] M. Mirea, Eur. Phys. J. A **4**, 335 (1999).
[24] M. Mirea, Phys. Rev. C **63**, 034603 (2001).
[25] M. Mirea, L. Tassan-Got, C. Stephan, C. O. Bacri, P. Stoica, and R. C. Bobulescu, J. Phys. G **31**, 1165 (2005).
[26] M. Mirea, L. Tassan-Got, C. Stephan, C. O. Bacri, and R. C. Bobulescu, Europhys. Lett. **73**, 705 (2006).
[27] M. Mirea, L. Tassan-Got, C. Stephan, C. O. Bacri, and R. C. Bobulescu, Phys. Rev. C **76**, 064608 (2007).
[28] J. Dobaczewski, W. Nazarewicz, T. R. Werner, J. F. Berger, C. R. Chinn, and J. Decharge, Phys. Rev. C **53**, 2809 (1996).
[29] M. Samyn, S. Goriely, and J. M. Pearson, Nucl. Phys. **A725**, 69 (2003).
[30] L. Bonneau, T. Kawano, T. Watanabe, and S. Chiba, Phys. Rev. C **75**, 054618 (2007).
[31] A. K. Kerman and N. Onishi, Nucl. Phys. **A361**, 179 (1981).
[32] M. Mirea, Mod. Phys. Lett. A **19**, 1809 (2003).
[33] J. A. Wheeler, *Niels Bohr and the Development of Physics*, edited by W. Pauli, L. Rosenfeld, and W. Weisskopf (Pergamon, London, 1955), p. 163.
[34] W. Norenberg, Phys. Lett. **B104**, 107 (1981).
[35] K. T. R. Davies, A. J. Sierk, and J. R. Nix, Phys. Rev. C **13**, 2385 (1976).
[36] J. W. Negele, S. E. Koonin, P. Moller, J. R. Nix, and A. J. Sierk, Phys. Rev. C **17**, 1098 (1978).
[37] M. Samyn, S. Goriely, P.-H. Heenen, J. M. Pearson, and F. Tondeur, Nucl. Phys. **A700**, 142 (2002).
[38] L. Brillard, A. G. Elayi, E. Hourani, M. Houssonnois, J. F. Le Du, and L.-H. Rosier, C. R. Acad. Sci. Ser. II **309**, 1105 (1989).
[39] M. Hussonnois, J. F. Le Du, L. Brillard, J. Dalmasso, and G. Ardisson, Phys. Rev. C **43**, 2599 (1991).
[40] E. Hourany, G. Berrier-Ronsin, A. Elayi, P. Hoffmann-Rothe, A. C. Mueller, L. Rosier, G. Rotbard, G. Renou, A. Liebe, D. N. Poenaru, and H. L. Ravn, Phys. Rev. C **52**, 267 (1995).
[41] R. K. Gupta, M. Horoi, A. Sandulescu, M. Greiner, and W. Scheid, J. Phys. G **19**, 2063 (1993).
[42] R. G. Lovas, R. J. Liotta, A. Insolia, K. Varga, and D. S. Delion, Phys. Rep. **294**, 265 (1998).
[43] J. R. Nix, Annu. Rev. Nucl. Sci. **22**, 65 (1972).
[44] K. T. R. Davies and J. R. Nix, Phys. Rev. C **14**, 1977 (1976).
[45] D. N. Poenaru, M. Ivascu, and D. Mazilu, Comput. Phys. Commun. **19**, 205 (1980).
[46] M. Brack, J. Damgaard, A. Jensen, H. Pauli, V. Strutinsky, and W. Wong, Rev. Mod. Phys. **44**, 320 (1972).
[47] D. N. Poenaru, M. Mirea, W. Greiner, I. Cata, and D. Mazilu, Mod. Phys. Lett. A **5**, 2101 (1990).
[48] D. Glas and U. Mosel, Nucl. Phys. **A264**, 268 (1985).
[49] R. M. Freeman, Z. Basrak, F. Haas, A. Hachem, G. A. Monnehan, A. Morsad, and M. Youlal, Phys. Rev. C **38**, 1081 (1988).
[50] T. Tazawa and Y. Abe, Phys. Rev. C **41**, R17 (1990).
[51] A. Thiel, J. Phys. G **16**, 867 (1990).
[52] M. Bender, P.-H. Heenen, and P.-G. Reinhard, Rev. Mod. Phys. **75**, 121 (2003).
[53] N. Dubray, H. Goutte, J. F. Berger, and J. P. Delaroche, Int. J. Mod. Phys. E **17**, 72 (2008).
[54] J. Skalski, Phys. Rev. C **77**, 064610 (2008).
[55] R. Y. Cusson and H. W. Meldner, Phys. Rev. Lett. **42**, 694 (1979).
[56] E. Kh. Yuldashbaeva, J. Libert, P. Quentin, and M. Girod, Phys. Lett. **B461**, 1 (1999).
[57] V. I. Abrosimov, D. M. Brink, A. Dellafiore, and F. Matera, Nucl. Phys. **A800**, 1 (2008).
[58] M. Urban and P. Schuck, Phys. Rev. A **73**, 013621 (2006).

[59] S. Nishiyama, Int. J. Mod. Phys. E **7**, 667 (1998).
[60] M. Mirea and R. K. Gupta, *Heavy Elements and Related New Phenomena*, edited by W. Greiner, and R. K. Gupta (World Scientific, Singapore, 1999), Chap. 19.
[61] D. S. Delion, S. Peltonen, and J. Suhonen, Phys. Rev. C **73**, 014315 (2006).
[62] D. S. Delion, A. Sandulescu, and W. Greiner, Phys. Rev. C **68**, 041303(R) (2003).
[63] M. Mirea, Rom. Rep. Phys. **59**, 523 (2007).
[64] S. Cwiok, J. Dudek, W. Nazarewicz, J. Skalski, and T. Werner, Comput. Phys. Commun. **46**, 379 (1987).
[65] H. C. Pauli, Phys. Rep. **7**, 35 (1973).
[66] M. Mirea, Phys. Rev. C **54**, 302 (1996).
[67] M. Mirea, Nucl. Phys. **A780**, 13 (2006).
[68] J. Maruhn and W. Greiner, Z. Phys. **251**, 431 (1972).
[69] L.-S. Geng, J. Meng, and T. Hiroshi, Chin. Phys. Lett. **24**, 1865 (2007).
[70] A. Diaz-Torres and W. Scheid, Nucl. Phys. **A757**, 373 (2005).